Epilepsia, 52(9):1570–1578, 2011
doi: 10.1111/j.1528-1167.2011.03247.x

FULL-LENGTH ORIGINAL RESEARCH

Positive shifts of the $GABA_A$ receptor reversal potential due to altered chloride homeostasis is widespread after status epilepticus

***Gleb Barmashenko, †Stefan Hefft, ‡Ad Aertsen, *Timo Kirschstein, and *Rüdiger Köhling**

***Oscar Langendorff Institute of Physiology, University of Rostock, Rostock, Germany; †Neurocenter, University Hospital Freiburg, Freiburg, Germany; and ‡Bernstein Center Freiburg, University of Freiburg, Freiburg, Germany**

Summary

Purpose: γ-Aminobutyric acid (GABA)ergic transmission plays an important role in the initiation of epileptic activity and the generation of ictal discharges. The functional alterations in the epileptiform hippocampus critically depend on GABAergic mechanisms and cation-chloride cotransporters.

Methods: To understand the cellular basis of specific functional alterations in the epileptic hippocampus, we studied physiologic characteristics and pharmacologically isolated evoked $GABA_A$ receptor–mediated inhibitory postsynaptic currents (IPSCs) recorded from principal neurons in hippocampal slices from status epilepticus (SE) and control rats using whole-cell and gramicidin perforated patch-clamp recordings.

Key Findings: Whereas the resting membrane potential and input resistance were not significantly different between control and epileptic tissue, the reversal potential (E_{GABA}) of IPSCs was significantly shifted to more positive values in SE rats with regard to the resting membrane potential. Pharmacologic experiments and quantitative reverse transcriptase polymerase chain reaction (RT-PCR) showed that the observed changes in the epileptic tissue were due to a decreased ratio of the main Cl^- extrusion transporter (K^+-Cl^- cotransporter, KCC2) to the main Cl^- uptake transporter (Na^+-K^+-$2Cl^-$ cotransporter, NKCC1).

Significance: Our results suggest that alterations of cation-chloride cotransporter functions, comprising a higher NKCC1 action, contribute to hyperexcitability within the hippocampus following SE.

KEY WORDS: Epilepsy, GABA, Gramicidin perforated patch-clamp, NKCC1, KCC2.

Epilepsy is one of the most common chronic neurologic disorders. It is characterized by both an increased synchronization of the neuronal network and a rise in cellular excitability. Traditionally, down-regulation of synaptic inhibition leading to an ''imbalance'' between excitation and inhibition and hence overexcitability of the ictogenic network is commonly proposed as an important underlying cellular mechanism for the generation of seizures (McCormick, 1989). There is increasing evidence, however, that γ-aminobutyric acid (GABA)ergic systems do not only subserve a dampening function in the brain, but may also have a region-specific proepileptic impact on neuronal networks, that is, McCormick demonstrated that focal application of GABA in human neocortex from patients with temporal lobe epilepsy (TLE) resulted in a depolarization of neurons (McCormick, 1989). Cohen et al. (2002) have observed similar GABA-mediated depolarizations in the subiculum of slices prepared from resected human epileptic hippocampus. Furthermore, in a 0-Mg^{2+} model of epilepsy, a depolarizing action of GABA was found to induce epileptiform network synchronization in the gamma band (Kohling et al., 2000).

Other investigations have shown that brain-derived neurotrophic factor (BDNF) mediated a loss of K^+-Cl^- cotransporter KCC2 (Rivera et al., 1999, 2002) in epilepsy. Spontaneously occurring $GABA_A$ receptor–mediated synaptic potentials in vitro can also be observed in neocortical slices of resected human temporal lobe tissue (Kohling et al., 1998). These, however, appear to mediate mainly hyperpolarizing potentials, although a reduction of depolarizing potentials could be observed during the initial phase of bicuculline application (Kohling et al., 1998). Finally, a positive shift of the $GABA_A$ receptor–equilibrium potential (E_{GABA}) following status epilepticus (SE) was observed in the dentate gyrus (Pathak et al., 2007), and this seems to go along with a similar shift in the deep entorhinal cortex (Bragin et al., 2009).

Accepted July 12, 2011.
Address correspondence to Timo Kirschstein, Oscar Langendorff Institute of Physiology, University of Rostock, 18057 Rostock, Germany. E-mail: timo.kirschstein@uni-rostock.de

Although positive shifts of E_{GABA} were described in the dentate gyrus (Pathak et al., 2007) as well as in the entorhinal cortex (Bragin et al., 2009), a comprehensive spatial description of the Cl^- homeostasis throughout all regions of the epileptic hippocampus is still missing. The aim of this investigation was thus to determine E_{GABA} in all subfields of the hippocampus following pilocarpine-induced SE and to elucidate its underlying mechanisms. Cation-chloride cotransporters play a key role in intracellular Cl^- regulation thus shaping GABAergic transmission (Kaila, 1994). Therefore, we also assessed the function of two major Cl^- regulators in hippocampal neurons: the Na^+-K^+-$2Cl^-$ cotransporter (usually type 1; NKCC1) and the K^+-Cl^- cotransporter (in neurons usually type 2; KCC2) mediating Cl^- uptake and Cl^- extrusion, respectively.

Materials and Methods

All experimental procedures were approved by the local ethics committee and were performed in accordance with the European Community Council directive of 24 November 1986 (S6 609 EEC) and the German guidelines for care und use of animals for experimental procedures.

Pilocarpine-induced status epilepticus

Sustained SE was induced in young male Wistar rats (130–140 g) at postnatal day 30. First, all animals received methyl scopolamine nitrate (1 mg/kg, i.p.) to reduce peripheral cholinergic effects. Afterwards 30-min pilocarpine was applied (340 mg/kg, i.p.) to induce SE, which was terminated 40 min after onset by injection of diazepam (4–10 mg/kg, i.p.; denoted as Pilo group). If SE did not develop within 60-min animals were reinjected (170 mg/kg, i.p.). The recordings were performed 7–14 days after pilocarpine treatment (or equivalently, after saline injection for control).

Slice preparation

Rats were deeply anesthetized with ketamine (80%) and xylazine (20%) and then decapitated. The brain was rapidly removed from the skull and immersed in ice-cold sucrose-based solution (87 mM NaCl, 25 mM $NaHCO_3$, 10 mM D-glucose, 75 mM sucrose, 2.5 mM KCl, 1.25 mM NaH_2PO_4, 0.5 mM $CaCl_2$, 7 mM $MgCl_2$, bubbled with 95% O_2 and 5% CO_2, pH 7.4). Sagittal hippocampal slices (300 μm) were cut on a Vibratome (Leica VT 1200S, Leica Microsystems, Wetzlar, Germany). Slices were incubated for 15 min in a storage/cutting solution at 34°C and then kept at room temperature. For recordings, the slices were transferred to a submerged recording chamber that was mounted under an upright microscope (Nikon, Tokyo, Japan) equipped with a 40× water immersion objective (N.A. = 0.8; Nikon). During the experiments, the chamber was perfused at a flow rate of 3 ml/min with oxygenated artificial cerebrospinal fluid (ACSF; 125 mM NaCl, 2.5 mM KCl, 1.25 mM NaH_2PO_4, 25 mM $NaHCO_3$, 25 mM D-glucose, 2 mM $CaCl_2$, 1 mM $MgCl_2$, pH 7.4). All recordings were performed at room temperature.

Stimulation and recording

Whole-cell gramicidin perforated patch-clamp recordings were performed from visually and electrophysiologically identified dentate gyrus granule cells (DGs), pyramidal neurons from *Cornu Ammonis* areas 1 and 3 (CA1, CA3, respectively), and the subiculum (Sub). Borosilicate patch electrodes (5–9 MΩ) were filled with a solution containing 35 mM K-gluconate, 110 mM KCl, 10 mM 4-(2-hydroxyethyl)-1-piperazineethanesulfonic acid (HEPES), 2 mM $MgCl_2$, 2 mM Na_2ATP, 10 mM ethylene glycol tetraacetic acid (EGTA) (pH 7.4). Subsequently, pipettes were back-filled with the same solution containing gramicidin prepared freshly prior to recording and kept on ice at most 3 h (10 μg/ml, dissolved in dimethyl sulfoxide (DMSO), final concentration of DMSO 0.1%; Sigma-Aldrich Chemie Gmbh, Munich, Germany). The intracellular Na^+ channel blocker lidocaine *N*-ethyl bromide (QX-314, 1 mM; Tocris Cookson, Bristol, United Kingdom) was added to this solution to verify the integrity of perforation. Physiologic membrane properties were estimated in current-clamp mode by applying depolarizing and hyperpolarizing current steps (600 ms duration).

$GABA_A$ receptor–mediated postsynaptic currents were isolated by addition of 6-cyano-7-nitroquinoxaline-2,3-dione (CNQX) (10 μM) and (2R)-amino-5-phosphonovaleric acid (D-AP5) (25 μM) to the ACSF to block excitatory transmission mediated by AMPA/kainate and *N*-methyl-D-aspartatic acid (NMDA) receptors, respectively. In the first set of experiments, $GABA_A$ receptor–mediated inhibitory postsynaptic currents (IPSCs) were evoked through a concentric bipolar electrode placed at a distance of 50–100 μm lateral to the recorded neuron with a stimulation rate of 0.1 Hz (20–100 μA, 100 μs duration). In a second set of experiments, spontaneous miniature $GABA_A$ receptor–mediated IPSCs were recorded by holding the neuron at its resting membrane potential. Patch-clamp recording was performed using an EPC10 patch-clamp amplifier, using a low-pass filter of 3 kHz, and a sample rate of 10 kHz. The series resistance compensation was about 70–80%. To identify the reversal potential of $GABA_A$ receptor–mediated currents (E_{GABA}), the holding potentials were systematically varied from −100 to −20 mV in 10-mV-steps. Membrane potential was verified after breaking the perforated patch following recording. Liquid junction potentials were not corrected for.

The drugs applied were 3-(aminosulfonyl)-5-(butylamino)-4-phenoxybenzoic acid (bumetanide), 4-chloro-*N*-furfuryl-5-sulfamoylanthranilic acid, 5-(aminosulfonyl)-4-chloro-2-([2-furanylmethyl]amino)benzoic acid (furosemide), 6-cyano-7-nitroquinoxaline-2,3-dione disodium salt hydrate (CNQX), 2-(3-carboxypropyl)-3-amino-6-(4

methoxyphenyl)-pyridazinium bromide (gabazine), and D-2-amino-5-phosphonopentanoic acid (D-AP5) (Sigma-Aldrich, Taufkirchen, Germany). Substances were prepared as stock solutions, frozen, finally thawed on the day of the experiment and added to ACSF to reach the desired final concentration.

Quantitative RT-PCR

Total RNA was isolated from pooled minislices, that is, slices only containing CA1, CA3, dentate gyrus or subiculum, respectively, using TRIZOL reagent. Total RNA was reverse-transcribed using Moloney murine leukaemia virus reverse transcriptase (200 U/μl) and RNasin Plus RNase inhibitor (40 U/μl; both Promega Corporation, Madison, WI, U.S.A.) in the presence of random hexamers (3 μg/μl) and dNTP Mix (10 mM each; Invitrogen, Carlsbad, CA, U.S.A.). Real-time PCR was performed using a reaction master mix consisting of 10× buffer, Mg^{2+} (Cf = 4 mM), deoxyribonucleotide triphosphates (Cf = 200 μM), Platinum Taq polymerase (0.6 U/20 μl reaction; Invitrogen), and SYBR Green (concentration as recommended by the manufacturer; Qiagen Inc., Valencia, CA, U.S.A.). The mastermix was aliquoted and cDNA and primers (Cf = 20 μmol) were added. The amplicons for NKCC1 and KCC2 were 150 and 147 bp, respectively (primers for NKCC1: GTCGCTGTATTCTTTAGCTCTG, ACGCTCATAAGTCATGGC; primers for KCC2: GCG GGATGCCCAGAAGTCTA, GATGCAGGCTCCAAAC AGAACA), and the amplicon for the housekeeping gene GAPDH (glyceraldehyde 3-phosphate dehydrogenase) was 150 bp (primers for GAPDH: CCGCAGCTAGGAA-TAATGGA, CCCTCTTAATCATGGCCTCA; all from TIB Molbiol, Berlin, Germany). Real-time PCR was done using the Mastercycler ep realplex software (Eppendorf, Hamburg, Germany) with cycling parameters 95°C for 2 min once, followed by 95°C for 30 s and 60°C for 45 s, with normalized fluorescence read at 59.7°C (521 nm) for 40 cycles. Single-product amplification was confirmed by melting curve and gel electrophoresis analysis. KCC2-mRNA and NKCC1-mRNA levels in all hippocampal regions were determined by comparison with GAPDH-mRNA as the mean of $2^{\Delta\Delta C_t}$ ± standard error of the mean (SEM), and then expressed as the ratio KCC2/NKCC1.

Western blot

The tissue samples (CA1, CA3, DG) were homogenized in lysis buffer (Tris 10 mM, NaCl 140 mM, EDTA 5 mM, Triton-X 1%, dithiothreitol 1 mM, KCl 75 mM, and proteinase inhibitors) and centrifuged at 21913 *g* at 4°C for 30 min. For immunoblotting, aliquots of the supernatant containing 50 μg of protein were subjected to 12% sodium dodecyl sulfate-polyacrylamide gel electrophoresis and immunoblotted onto polyvinylidene fluoride membranes (GE Healthcare, Munich, Germany). The residual binding sites on the membrane were blocked by incubation with 5% milk powder in phosphate-buffered saline containing Tween-20 (PBST) for 1 h, followed by incubation with the rabbit anti-KCC2 antibodies (1:1,000; Abcam, Cambridge, United Kingdom) overnight. The blots were washed in PBST, and then incubated with the secondary antibody using horseradish peroxidase-conjugated anti-rabbit IgG (GE Healthcare) for 1 h, which was detected using chemiluminescence (GE Healthcare).

Statistics

Data were expressed as means ± SEM. Statistical analysis was done using SIGMASTAT software (Systat Software, Erkrath, Germany) performing Student's *t*-test and one-way-analysis of variance (ANOVA). Differences were considered significant when $p < 0.05$.

Results

In the first set of experiments, we compared the basic electrophysiologic properties and threshold parameters of neurons from control (Fig. 1A) and epileptic rats (Fig. 1B) in current-clamp mode by applying depolarizing and hyperpolarizing current steps (600 ms duration, Fig. 1). The average resting membrane potential, input resistance, membrane time constant, and cell capacitance were not significantly different between neurons recorded from the pilocarpine-treated and control groups (Table 1). Although all cells were regular firing, spike frequency was significantly higher in neurons from rats after SE—compared to control animals—in regions CA1 and CA3 (Table 1), indicating a higher intrinsic excitability of these neurons.

In the second set of experiments, we compared the maximum amplitudes of electrically evoked IPSCs in epileptic and control rats. Monosynaptic $GABA_A$ receptor ($GABA_AR$) mediated currents were recorded using the gramicidin perforated patch-clamp method at holding potentials between −100 mV and −20 mV (Fig. 1A). IPSCs recorded in the presence of CNQX (10 μM) and D-AP5 (25 μM) were completely blocked by gabazine (30 μM), confirming that they were mediated by $GABA_A$ receptors (not shown). In all regions, reversal potentials of $GABA_A$ receptor–mediated currents (E_{GABA}) in neurons from epileptic animals were significantly shifted to more positive values compared to controls (Table 1). Whether E_{GABA} renders inhibitory currents depolarizing, depends on the actual resting membrane potential (RMP). Table 1 shows that in controls, E_{GABA} is more negative than RMP in all regions of the hippocampus resulting in hyperpolarizing inhibitory postsynaptic potential (IPSP) evoked at our stimulation paradigm used here. In contrast, in neurons recorded after SE, E_{GABA} becomes more positive than RMP (which should result in depolarizing $GABA_AR$–mediated potentials). This difference between RMP and E_{GABA} reached significance for E_{GABA} of recorded currents in the dentate gyrus, and the subiculum (Table 1).

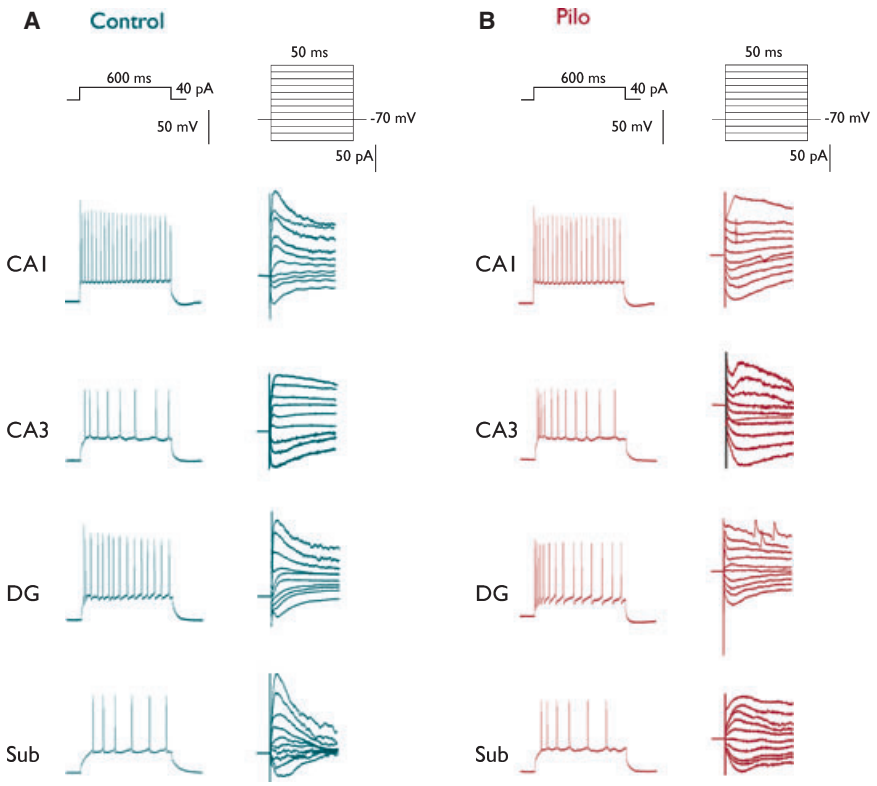

Figure 1.
Reversal potentials of $GABA_A$ receptor–mediated currents and firing behavior of neurons from control and epileptic tissue. Physiologic membrane properties as well as firing properties were estimated in the current-clamp mode by applying depolarizing and hyperpolarizing current steps (600 ms duration). Sample traces of hippocampal neurons depolarized beyond firing threshold by current injection from a control (**A**) and an epileptic animal (**B**) one week after SE. Sample traces of the electrically evoked $GABA_A$ receptor–mediated postsynaptic currents in hippocampal cells from control and epileptic animals. Monosynaptic $GABA_A$ receptor–mediated postsynaptic currents were evoked by focal electrical stimulation via a concentric bipolar electrode under continuous blockade of glutamatergic transmission using CNQX (10 μM) and D-AP5 (25 μM). Holding potentials were systematically varied from −100 to −20 mV in 10-mV-steps. Action potential currents occasionally occurring at depolarizing pulses were truncated.

Table 1. Intrinsic properties and E_{GABA} of hippocampal neurons

	n	Resting membrane potential, mV	Input resistance, MΩ	Time constant, ms	Spike frequency, s^{-1}	E_{GABA}, mV
Control						
CA1	7	−68.0 ± 2.3	122 ± 31	22 ± 4	19 ± 2	−68.9 ± 1.8
CA3	6	−64.0 ± 2.3	117 ± 17	26 ± 7	18 ± 2	−70.0 ± 2.2
DG	15	−71.7 ± 1.9	177 ± 26	14 ± 6	13 ± 2	−74.6 ± 1.8**
Sub	6	−74.3 ± 0.6	184 ± 47	13 ± 7	12 ± 1	−75.3 ± 2.0**
Pilo						
CA1	11	−68.5 ± 2.1	113 ± 18	23 ± 5	34 ± 3***	−63.3 ± 1.5***
CA3	11	−68.4 ± 1.5	98 ± 21	24 ± 9	28 ± 3*	−64.2 ± 2.3*
DG	13	−73.4 ± 1.2	140 ± 34	12 ± 6	20 ± 5	−66.7 ± 0.8***
Sub	9	−74.2 ± 2.5	176 ± 22	13 ± 8	21 ± 4	−65.3 ± 1.7***

n, number of cells.
Data are given as means ± SEM.
*$p < 0.05$ between Control and Pilo.
**$p < 0.01$ between E_{GABA} and resting membrane potential.
***$p < 0.01$ between Control and Pilo.

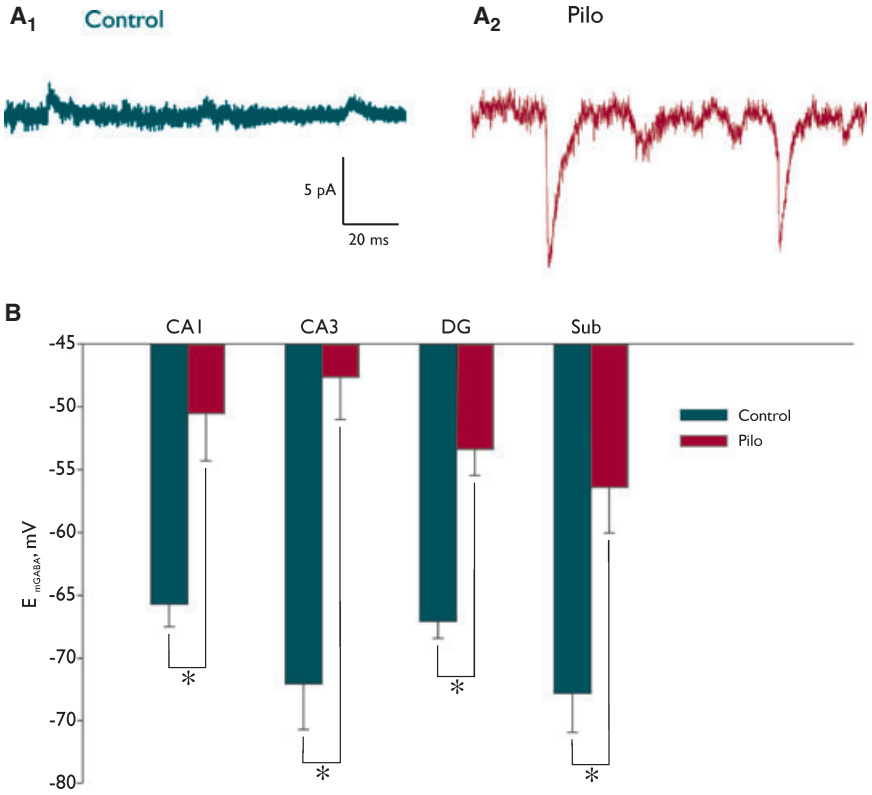

Figure 2.
Miniature $GABA_A$ receptor–mediated currents in neurons from control and epileptic (Pilo) rats. (**A**) Sample traces of miniature $GABA_A$ receptor–mediated currents in CA3 neurones from control (**A_1**) and epileptic (**A_2**) rats. When the holding potential was equal to the resting membrane potential of the cell we observed the inhibitory miniature $GABA_A$ receptor–mediated currents in control and excitatory miniature $GABA_A$ receptor–mediated currents in epileptic tissue. (**B**) In order to find the reversal potential of the miniature $GABA_A$ receptor–mediated currents (E_{mGABA}), holding potentials were systematically varied from −90 mV to −40 mV in 10-mV-steps. In neurons from epileptic rats, E_{mGABA} was shifted toward more positive values compared to neurons from control rats in all hippocampal regions ($p < 0.05$, $n = 4$ for all regions).

Next, we asked if this shift of the $GABA_A$ receptor reversal potential is also present in spontaneous miniature IPSCs. Therefore, we clamped the cells at their individual resting membrane potential and pharmacologically isolated GABAergic spontaneous synaptic events. As shown in Fig. $2A_1$, in control neurons small outward currents occurred as would be expected for inhibitory miniature IPSCs. However, in slices from epileptic rats, large inward currents were observed (Fig. $2A_2$). Upon variation of the holding potential, the reversal potential for miniature IPSCs (E_{mGABA}) was determined. Under these conditions, E_{mGABA} was significantly shifted toward more positive values in all four hippocampal regions (Fig. 2B), which strikingly confirmed our results with evoked $GABA_A$ receptor–mediated currents.

In search of possible mechanisms responsible for the observed differences in E_{GABA}, we repeated the experiments in the presence of bumetanide (10 μM), a selective blocker for the net inward chloride transporter NKCC1, or furosemide (20 μM), a blocker of the outward transporter KCC2 at concentrations we used here (Russell, 2000). Both drugs were applied, sequentially and additively, to assess the effect of failure of the main chloride transporters, NKCC1 and KCC2, on E_{GABA}. Fig. 3 shows the averaged E_{GABA} in SE and control rats recorded for each single neuron measured in the different subfields. Adding bumetanide alone, the resulting specific NKCC1 block did not alter E_{GABA} in control rats, but significantly shifted E_{GABA} to more negative values in CA1 and CA3 pyramidal neurons recorded from pilocarpine-treated animals (Fig. 3, Table 2), suggesting that NKCC1 plays little role in determining E_{GABA} under control conditions, but significantly contributes to E_{GABA} in epileptic tissue. Additional application of the KCC2 blocker furosemide shifted E_{GABA} significantly to more positive values in neurons from both control and SE animals. Hence, KCC2 influences chloride homeostasis in

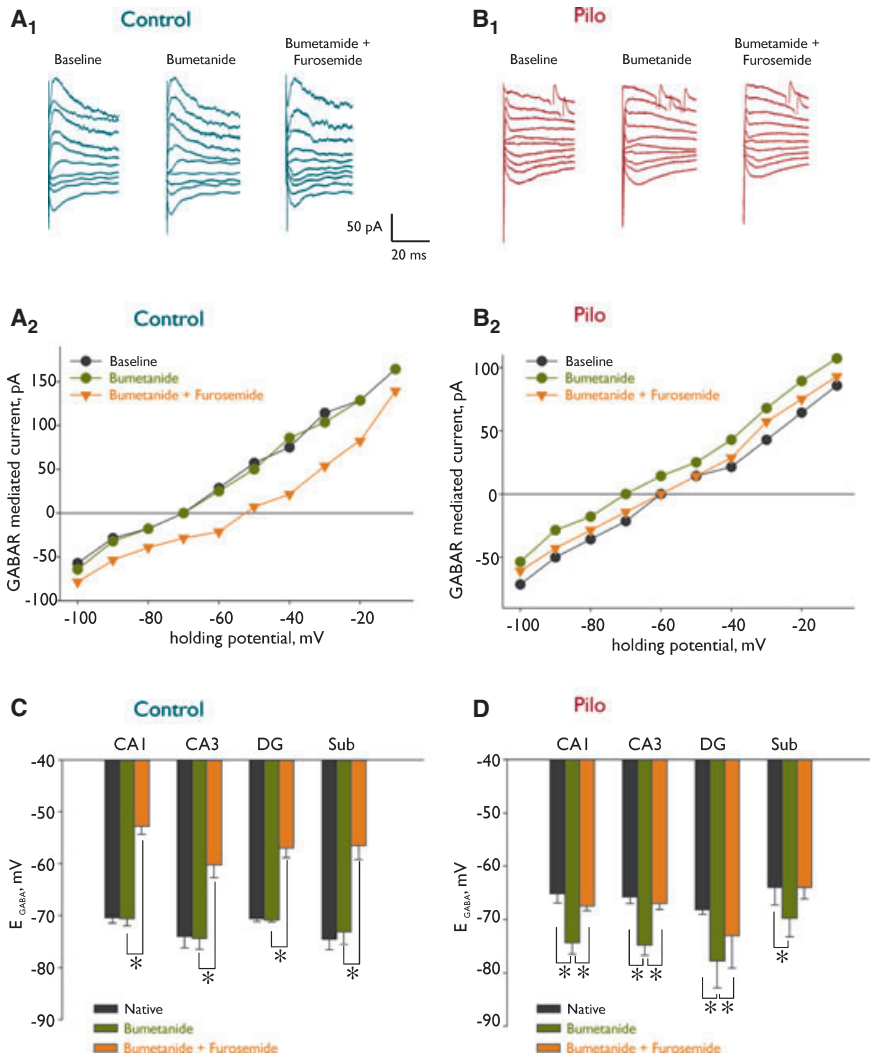

Figure 3.
Differential effects of bumetanide and furosemide on the GABA$_A$R–mediated currents in control and epileptic tissue. (**A**, **B**) Sample traces (**A**) and corresponding current-voltage curves (**B**) of the electrically evoked GABA$_A$ receptor–mediated postsynaptic currents in neurons from control (**A$_1$**, **B$_1$**) and epileptic (**A$_2$**, **B$_2$**) rats. Holding potentials were systematically varied from −100 mV to −20 mV in 10-mV-steps. Note the E_{GABA} shift in positive direction with furosemide (KCC2 block) in control rats and the E_{GABA} shift in negative direction with bumetanide (NKCC1 block) in epileptic rats. Action potential currents occasionally occurring at depolarizing pulses were truncated. (**C**) Bar graphs of mean values ± SEM of E_{GABA} in cells of hippocampal regions CA1, CA3, dentate gyrus (DG), and subiculum (Sub) from control animals. The selective blocker of the inward chloride-transporter NKCC1, bumetanide (10 μM), has no significant effect on E_{GABA} in any of the regions investigated. Additional application of the outward chloride-transporter KCC2-inhibitor furosemide (20 μM) shifts E_{GABA} to more positive values ($p < 0.001$ in CA1, DG, und Sub, $p < 0.005$ in CA3, ANOVA). (**D**) Bar graphs of mean values ± SEM of E_{GABA} in cells of hippocampal regions CA1, CA3, dentate gyrus (DG), and subiculum (Sub) from rats 1 week after pilocarpine-induced SE. The NKCC1 inhibitor significantly shifts E_{GABA} to more negative values ($p < 0.01$ in CA1, $p < 0.005$ in CA3, $p < 0.05$ in DG, $p < 0.001$ in Sub, ANOVA). With concomitant blockade of the KCC2 transporter using furosemide (20 μM), E_{GABA} is shifted back to its original level, again significantly in CA1, CA3, and DG ($p < 0.02$ in CA1, $p < 0.01$ in CA3, $p < 0.05$ in DG, ANOVA).

both control and pilocarpine-treated rats when chloride inward transport was reduced by prior application of the NKCC1 blocker bumetanide.

Given that the shift of E_{GABA} in epileptic tissue was due to an increased function of NKCC1 and/or depressed function of KCC2, we analyzed these two main chloride

Table 2. Effect of cation-chloride cotransporters on E_{GABA}

	n	Baseline	Bumetanide	Bumetanide + furosemide
Control				
CA1	5	−70.4 ± 1.0	−70.6 ± 1.4	−52.8 ± 1.5****
CA3	5	−74.0 ± 2.2	−74.4 ± 2.1	−60.2 ± 2.5****
DG	5	−70.6 ± 0.5	−70.8 ± 0.4	−57.0 ± 1.9****
Sub	6	−74.5 ± 2.1	−73.2 ± 2.3	−56.5 ± 2.7****
Pilo				
CA1	5	−65.2 ± 1.7	−74.4 ± 2.1**	−67.4 ± 0.9
CA3	5	−65.8 ± 1.2	−74.8 ± 1.9**	−67.0 ± 1.1
DG	5	−68.2 ± 0.8	−77.8 ± 5.0**	−73.0 ± 6.1
Sub	5	−64.0 ± 3.3	−69.8 ± 3.4**	−64.2 ± 2.3

n, number of cells.

Data are given as means ± SEM; E_{GABA} was measured with successive and additive blockade of NKCC1, and KCC2 transporters using bumetanide (10 μM), and combined application of bumetamide (10 μM) + furosemide (20 μM).

*$p < 0.05$ between bumetanide and combined bumetanide/furosemide.

**$p < 0.05$ between bumetanide and combined bumetanide/furosemide as well as between bumetanide and baseline.

***$p < 0.01$ between combined bumetanide/furosemide and baseline.

transporters on the transcriptional level. Indeed, we found a KCC2 down-regulation as well as an NKCC1 up-regulation in all hippocampal regions when compared to the housekeeping gene *GAPDH*. Therefore, the amplification plots in Fig. 4A demonstrate a rightward shift of KCC2 (circles) and a leftward shift of NKCC1 (triangles) in all hippocampal regions taken from epileptic rats (closed symbols) as compared to control tissue samples (open symbols). This alteration, however, becomes even more evident, when the ratio of KCC2-mRNA to NKCC1-mRNA was determined (Fig. 4B). In all regions of the epileptic hippocampus tested, this ratio was significantly decreased, and thus, this reduction of KCC2 and up-regulation of NKCC1 may conceivably contribute to the shift of E_{GABA} toward positive values in epileptic tissue. Western blot analysis confirmed the reduction of KCC2 protein in CA1, CA3, and dentate gyrus (Fig. 4C). A reliable identification of NKCC1 staining was precluded by the lack of specificity of the NKCC1 antibodies available to us.

Discussion

The present study demonstrates that in the pilocarpine model of temporal lobe epilepsy, the reversal potential of $GABA_AR$–mediated currents was shifted to more positive values in all subfields tested. These changes may contribute to hyperexcitability and abnormal synchronization within the entire epileptic hippocampus. These results corroborate previous results showing alterations of GABA function, and in particular a positive shift of E_{GABA} in dentate gyrus granule cells 1 week after pilocarpine-induced SE (Pathak et al., 2007; Teichgraber et al., 2009), and expands this finding to the entire hippocampus. Crucially, in our study, the positive shift of E_{GABA} was also found at the output region, the subiculum, where GABAergic potentials were suggested to be depolarizing in neurons recorded in tissue obtained from patients with mesial temporal lobe epilepsy (MTLE) (Cohen et al., 2002; Huberfeld et al., 2007). A similar observation was found in nigral dopaminergic neurons, where it is thought to occur by down-regulation of KCC2 (Gulacsi et al., 2003). Hence, our results may be caused by a change in neuronal expression of the cation-chloride cotransporters in epileptic rats toward levels found in immature neurons. NKCC1 (Cl^--uptake) and KCC2 (Cl^--extrusion) are the most important chloride transporters in cortical neurons and represent thus the main regulators of chloride homeostasis (Kaila, 1994; Delpire, 2000). Although GABA is the main inhibitory transmitter in the adult brain, GABAergic transmission is excitatory during early postnatal development (Ben Ari, 2002). The different action of GABA results from a reversed Cl^- concentration gradient with higher intracellular Cl^- concentration in immature neurons. The developmental shift to an inhibitory action of GABA is a consequence of a decrease of NKCC1 and concomitant increase of KCC2 expression (Delpire, 2000; Vu et al., 2000; Ikeda et al., 2003). Vardi et al. (2000) demonstrated that the differential expression of KCC2 or NKCC1 in various types of cells of the retina led to corresponding opposite effects of GABA: NKCC1 expression being linked to depolarizing action of GABA, whereas KCC2 having the opposite effect.

Our results demonstrate that changes in $GABA_AR$–mediated currents correlate with an altered action of cation-chloride cotransporters in epileptic rats. This suggests that the elevated level of intracellular Cl^- in epileptic rats could be responsible for the differences observed. Bumetanide, the selective inhibitor of NKCC1 (at 10 μM) induced a significantly negative shift in E_{GABA} in epileptic, but not in control rats. These results indicated that the balance between inward and outward Cl^- cotransporters was altered in the entire hippocampus of SE rats, with NKCC1 bearing the main impact on E_{GABA} in neurones recorded in tissue, after it has been subjected to pilocarpine-induced SE. Conversely, KCC2 is the main determinant under physiologic conditions. This alteration seems to be reminiscent of the situation in immature neurons: increased NKCC1 and decreased KCC2 expression compared to mature neurons (Kakazu et al., 1999; Rivera et al., 1999; Mikawa et al., 2002; Stein & Nicoll, 2003; Yamada et al., 2004). The altered function of NKCC1 in particular might be a compensatory mechanism triggered by the adjustments necessary to address the differences in neuronal activity caused by SE. Such activity-dependent changes related to KCC2 expression were shown in hippocampal neurons (Rivera et al., 2004). Interestingly, the combined block of both transporters led to a marked positive shift of E_{GABA} in control conditions, but to significantly less positive one in cells from epileptic rats. Because both transporter types are

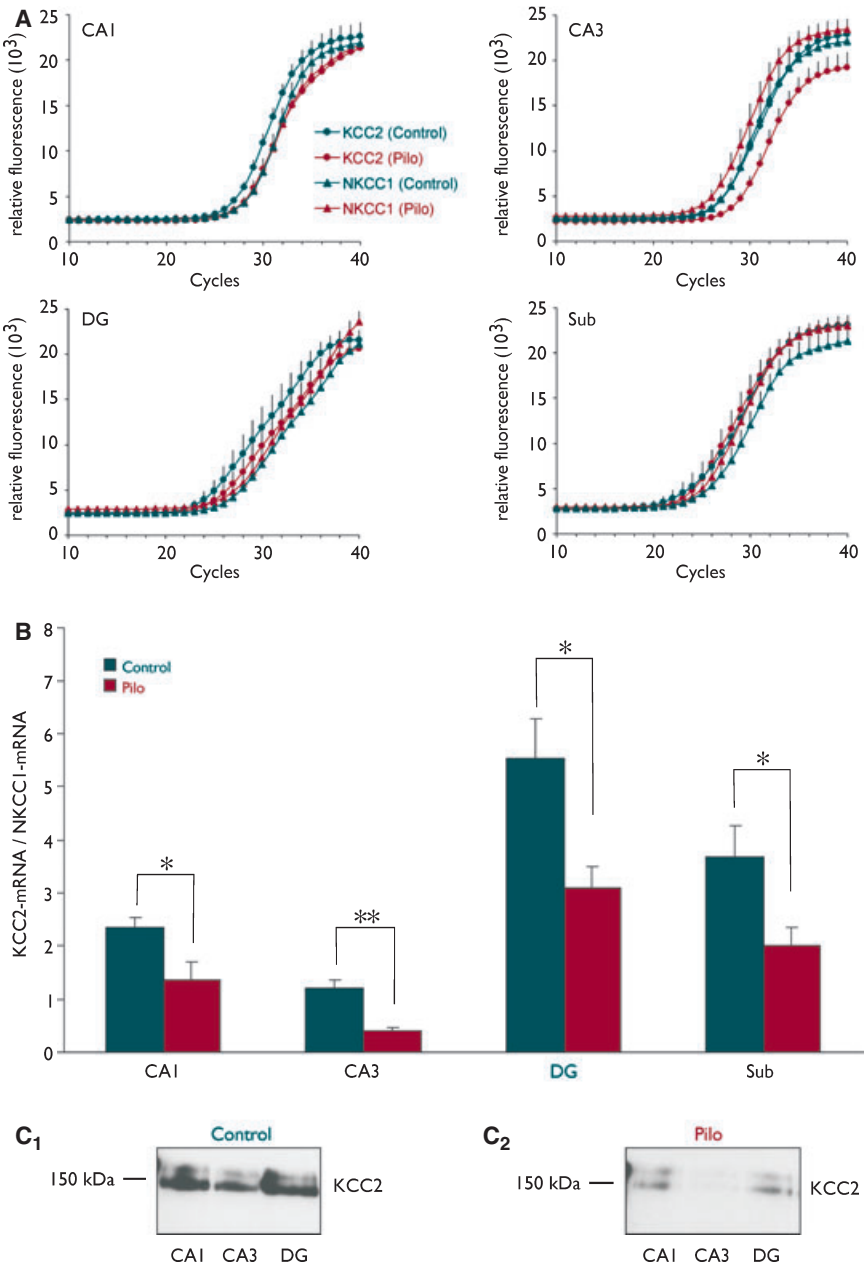

Figure 4.
Quantitative reverse transcriptase polymerase chain reaction (RT-PCR) reveals KCC2 down-regulation and NKCC1 up-regulation in epileptic tissue. (**A**) RT-PCR reveals a leftward shift of the amplification plots of NKCC1 (i.e., increased expression) and a rightward shift of the amplification plots of KCC2 (i.e., decreased expression) in epileptic tissue as compared to controls. (**B**) Bar graphs of mean values ± SEM of the ratio KCC2-mRNA/NKCC1-mRNA of hippocampal regions CA1, CA3, dentate gyrus (DG), subiculum (Sub) from rats 1 week after pilocarpine-induced SE. In all regions, this ratio is significantly reduced in epileptic tissue (n = 8 for CA1 and CA3, n = 12 for DG, n = 14 for Sub) as compared to control (n = 9 for CA1 and CA3, n = 14 for DG, n = 12 for Sub) indicating a KCC2 down-regulation and NKCC1 up-regulation in epileptic tissue ($p < 0.05$ in CA1, DG und Sub, $p < 0.01$ in CA3, *t*-test). (**C**) Western blot shows the reduction of KCC2 protein in CA1, CA3, and dentate gyrus of Pilo tissue (**C_2**) as compared to control tissue (**C_1**).
Epilepsia © ILAE

dysfunctional under these conditions, E_{GABA} should be similar in both groups if transporters were the only mechanisms determining it. Hence, some other mechanism apart from the transporters is also involved in generating a disparity of E_{GABA}. Incidentally, this mechanism in cells from epileptic rats is one that tends to bring E_{GABA} to levels found control cells whose transporters are still intact. This points to a compensatory process counteracting the transporter function changes in epileptic neurons.

Taken together, our results confirm and extend previously published ones: Here, we show that depolarizing actions of $GABA_A$ receptor–mediated currents are present throughout all subfields of the hippocampus (DG, CA1, CA3, and subiculum), at least during early epileptogenesis, which supports previous investigations restricted to dentate gyrus granule cells (Pathak et al., 2007) and the entorhinal cortex (Bragin et al., 2009). As a result, spatial or temporal summation of depolarizing IPSPs and concomitant excitatory postsynaptic potential (EPSP) are likely to occur. Whether depolarizing IPSPs are actually excitatory or shunting (and hence still inhibiting), will depend on the level of both input resistance change and size of concomitant inward synaptic currents. Nevertheless, the functional change observed here, together with a breakdown of the

filter function of the dentate gyrus (Pathak et al., 2007), reduced $GABA_B$ receptor function (Teichgraber et al., 2009), and an entorhinal cortex strongly susceptible to GABAergic excitation (Bragin et al., 2009), may play a key role at least during early stages of epileptogenesis of TLE.

Whether a depolarizing action of $GABA_A$ receptor–mediated currents due to a shift of E_{GABA} does occur in humans, as suggested by microelectrode recordings performed in slices prepared from human epileptic hippocampus, still needs to be confirmed.

Acknowledgments

This study was funded by grants from the German Federal Ministry for Education and Science (BMBF, grant no. 01GQ0751) and the Medical Faculty of the University of Rostock (FORUN). The authors gratefully acknowledge Katrin Porath, Ulrike Mikkat, and Tina Sellmann for their excellent technical assistance.

Disclosure

None of the authors has any conflict of interest to disclose. We confirm that we have read the Journal's position on issues involved in ethical publication and affirm that this report is consistent with those guidelines.

References

Ben Ari Y. (2002) Excitatory actions of GABA during development: the nature of the nurture. *Nat Rev Neurosci* 3:728–739.

Bragin DE, Sanderson JL, Peterson S, Connor JA, Muller WS. (2009) Development of epileptiform excitability in the deep entorhinal cortex after status epilepticus. *Eur J Neurosci* 30:611–624.

Cohen I, Navarro V, Clemenceau S, Baulac M, Miles R. (2002) On the origin of interictal activity in human temporal lobe epilepsy in vitro. *Science* 298:1418–1421.

Delpire E. (2000) Cation-chloride cotransporters in neuronal communication. *News Physiol Sci* 15:309–312.

Gulacsi A, Lee CR, Sik A, Viitanen T, Kaila K, Tepper JM, Freund TF. (2003) Cell type-specific differences in chloride-regulatory mechanisms and GABA(A) receptor-mediated inhibition in rat substantia nigra. *J Neurosci* 23:8237–8246.

Huberfeld G, Wittner L, Clemenceau S, Baulac M, Kaila K, Miles R, Rivera C. (2007) Perturbed chloride homeostasis and GABAergic signaling in human temporal lobe epilepsy. *J Neurosci* 27:9866–9873.

Ikeda M, Toyoda H, Yamada J, Okabe A, Sato K, Hotta Y, Fukuda A. (2003) Differential development of cation-chloride cotransporters and Cl− homeostasis contributes to differential GABAergic actions between developing rat visual cortex and dorsal lateral geniculate nucleus. *Brain Res* 984:149–159.

Kaila K. (1994) Ionic basis of GABAA receptor channel function in the nervous system. *Prog Neurobiol* 42:489–537.

Kakazu Y, Akaike N, Komiyama S, Nabekura J. (1999) Regulation of intracellular chloride by cotransporters in developing lateral superior olive neurons. *J Neurosci* 19:2843–2851.

Kohling R, Lucke A, Straub H, Speckmann EJ, Tuxhorn I, Wolf P, Pannek H, Oppel F. (1998) Spontaneous sharp waves in human neocortical slices excised from epileptic patients. *Brain* 121(Pt 6):1073–1087.

Kohling R, Vreugdenhil M, Bracci E, Jefferys JG. (2000) Ictal epileptiform activity is facilitated by hippocampal GABAA receptor-mediated oscillations. *J Neurosci* 20:6820–6829.

McCormick DA. (1989) GABA as an inhibitory neurotransmitter in human cerebral cortex. *J Neurophysiol* 62:1018–1027.

Mikawa S, Wang C, Shu F, Wang T, Fukuda A, Sato K. (2002) Developmental changes in KCC1, KCC2 and NKCC1 mRNAs in the rat cerebellum. *Brain Res Dev Brain Res* 136:93–100.

Pathak HR, Weissinger F, Terunuma M, Carlson GC, Hsu FC, Moss SJ, Coulter DA. (2007) Disrupted dentate granule cell chloride regulation enhances synaptic excitability during development of temporal lobe epilepsy. *J Neurosci* 27:14012–14022.

Rivera C, Voipio J, Payne JA, Ruusuvuori E, Lahtinen H, Lamsa K, Pirvola U, Saarma M, Kaila K. (1999) The K+/Cl− co-transporter KCC2 renders GABA hyperpolarizing during neuronal maturation. *Nature* 397:251–255.

Rivera C, Li H, Thomas-Crusells J, Lahtinen H, Viitanen T, Nanobashvili A, Kokaia Z, Airaksinen MS, Voipio J, Kaila K, Saarma M. (2002) BDNF-induced TrkB activation down-regulates the K+-Cl− cotransporter KCC2 and impairs neuronal Cl− extrusion. *J Cell Biol* 159:747–752.

Rivera C, Voipio J, Thomas-Crusells J, Li H, Emri Z, Sipila S, Payne JA, Minichiello L, Saarma M, Kaila K. (2004) Mechanism of activity-dependent downregulation of the neuron-specific K-Cl cotransporter KCC2. *J Neurosci* 24:4683–4691.

Russell JM. (2000) Sodium-potassium-chloride cotransport. *Physiol Rev* 80:211–276.

Stein V, Nicoll RA. (2003) GABA generates excitement. *Neuron* 37:375–378.

Teichgraber LA, Lehmann TN, Meencke HJ, Weiss T, Nitsch R, Deisz RA. (2009) Impaired function of GABA(B) receptors in tissues from pharmacoresistant epilepsy patients. *Epilepsia* 50:1697–1716.

Vardi N, Zhang LL, Payne JA, Sterling P. (2000) Evidence that different cation chloride cotransporters in retinal neurons allow opposite responses to GABA. *J Neurosci* 20:7657–7663.

Vu TQ, Payne JA, Copenhagen DR. (2000) Localization and developmental expression patterns of the neuronal K-Cl cotransporter (KCC2) in the rat retina. *J Neurosci* 20:1414–1423.

Yamada J, Okabe A, Toyoda H, Kilb W, Luhmann HJ, Fukuda A. (2004) Cl− uptake promoting depolarizing GABA actions in immature rat neocortical neurones is mediated by NKCC1. *J Physiol* 557:829–841.